Synthesis of POSS-Terminated Polycyclooctadiene Telechelics via Ring-Opening Metathesis Polymerization

Lei Li,[1] Chongyin Zhang,[2] Sixun Zheng[1]

[1]Department of Polymer Science and Engineering and the State Key Laboratory of Metal Matrix Composites, Shanghai Jiao Tong University, Shanghai 200240, People's Republic of China
[2]Shanghai Aerospace Equipment Manufacture, China Aerospace Science and Technology Corporation, Shanghai 200245, People's Republic of China
Correspondence to: S. Zheng (E-mail: szheng@sjtu.edu.cn)

Received 14 June 2016; accepted 6 September 2016; published online 21 September 2016
DOI: 10.1002/pola.28360

ABSTRACT: In this contribution, we reported the synthesis of a series of POSS-terminated polycyclooctadiene (PCOD) telechelics via ring-opening metathesis polymerization (ROMP) approach. Toward this end, 1,4-diPOSS-but-2-ene was synthesized via copper-catalyzed Huisgen cycloaddition reaction (i.e., click chemistry); it was then used as a chain transfer agent (CTA) for the ROMP of cyclooctadiene. The ROMP was carried out with Grubbs second generation catalyst and the POSS-terminated PCOD telechelics with variable lengths of PCOD were obtained by controlling the molar ratios of CTA to cyclooctadiene. All the POSS-terminated PCOD telechelics in bulks were microphase-separated; the morphologies were quite dependent on the lengths of PCOD midchains. The POSS end groups can promote the crystallization of PCOD chains at room temperature, which was in marked contrast to the case of plain PCOD. Compared to the plain PCOD, the POSS-terminated PCOD telechelics displayed improved thermal stability and surface hydrophobicity. © 2016 Wiley Periodicals, Inc. J. Polym. Sci., Part A: Polym. Chem. **2017**, *55*, 223–233

KEYWORDS: telechelics; ROMP; self-assembly; networks

INTRODUCTION Polyhedral oligomeric silsesquioxanes (POSS) are a class of important building blocks for the preparation of organic−inorganic hybrid materials.[1–3] It is realized that POSS-containing polymers can display some excellent comprehensive properties through the synergism of the inorganic and organic components. Generally, POSS are incorporated into organic polymers via chemical approaches. The formation of chemical linkages between POSS and organic polymers are critical to suppress the macroscopic phase separation of POSS in organic matrices. Depending on the number of reactive or polymerizable groups in POSS macromers, various chemical approaches such as reactive grafting, copolymerization and macromolecular reaction can be employed to introduce POSS cages into organic polymers. For instance, monofunctional POSS macromers can be either grafted onto polymer chains by radical copolymerization (or reactive grafting).[4,5] Difunctional POSS macromers can be incorporated into main chains of polymers to form the linear organic−inorganic polymers.[6,7] Multifunctional POSS macromers can be used as the nanosized crosslinking agents of the hybrid networks or cores of star-like polymers.[8,9]

POSS-terminated telechelics polymers represent a class of interesting architectures which contain associating "sticker" groups at the ends of polymer chains and thus display some specific topologies and self-assembly behavior.[10–14] Mather et al.[5,15] first reported the synthesis of heptacyclohexyl POSS-terminated poly(ethylene glycol) (PEG) telechelics via the reaction of isocyanatopropyl dimethylsilycyclohexyl-POSS and PEG. It was found that the POSS cages at the ends of chains altered the thermomechanical properties of poly(ethylene oxide). More importantly, the POSS-terminated PEG telechelics displayed the rheological behavior of physically crosslinked networks. Zeng et al.[10] utilized copper-catalyzed Huisgen cycloaddition reaction (i.e., click chemistry) between 3-azidopropylhepta (3,3,3-trifluoropropyl) POSS and dialkyne-terminated PEG to obtain POSS-terminated PEG telechelics. Owing to the POSS–POSS interactions, the organic−inorganic PEO telechelics were capable of forming a physically-crosslinked network, which was interpenetrated with poly(*N*-vinylpropylacryamide) (PNIPAAm) hydrogels. As a consequence, the swelling ratio and thermoresponsive properties of the modified PNIPAAm hydrogels were significantly improved. Recently, Zhang and Mueller reported the synthesis of POSS-terminated polystyrene (PS) telechelics via the combination of atom transfer radical polymerization and copper-catalyzed Huisgen cycloaddition reaction. They first synthesized bromine-terminated PS homopolymers, the end bromine atoms of which were then substituted with azido groups and then the azido-terminated PS was allowed to react with the

POSS macromer bearing single alkynyl group.[16] More recently, Wang et al.[17] explored an end-group-first approach to synthesize POSS-terminated poly(*N*-isopropylacrylamide) (PNIPAAm) telechelics. In this approach, a diPOSS-trithiocarbonate was synthesized and then used as a chain transfer agent (CTA) for the reversible addition–fragmentation chain transfer (RAFT) polymerization of NIPAAm monomer. This strategy was in marked contrast to the previous approaches that the ends of existing polymer chains were postcapped with POSS cages. By controlling the molar ratio of CTA and NIPAAm monomer, the POSS-terminated PNIPAAm telechelics with different lengths of PNIPAAm chains were obtained; the physical hydrogels resulting from the POSS-terminated PNIPAAm telechelics displayed improved thermoresponsive properties.

Ring-opening metathesis polymerization (ROMP) is a class of important living polymerization technique, which possesses high efficiency; the Grubbs' catalyst has excellent tolerance of functional groups.[18–22] Depending on the design of chain transfer agent (CTA) together with the uses of a variety of monomers, ROMP can be used to synthesize the polymers with desired macromolecular architectures.[23–36] To the best of our knowledge, nonetheless, the synthesis of POSS-terminated telechelic polymers via ROMP approach has not been reported. In this work, we explored to synthesize POSS-terminated polycyclooctadiene (PCOD) telechelics via ROMP approach. Toward this end, 1,4-diPOSS-but-2-ene was first synthesized via copper-catalyzed Huisgen cycloaddition reaction (i.e., click chemistry); it was then used as a chain transfer agent (CTA) for the ROMP of cyclooctadiene. The ROMP was performed with Grubbs second generation catalyst and POSS-terminated PCOD telechelics with variable lengths of PCOD were obtained by controlling the molar ratios of CTA to cyclooctadiene. The morphologies and thermal properties of the POSS-terminated PCOD telechelics were addressed on the basis of transmission electron microscopy (TEM), differential scanning calorimetry (DSC) and thermogravimetric analysis (TGA). The surface properties were investigated by the static contact angle measurements.

EXPERIMENTAL

Materials

Phenyltrimethoxysilane [$C_6H_5Si(OMe)_3$] was purchased from Zhejiang Chemical Technology, China. 3-Bromopropyltrichlorosilane, Grubbs second generation catalyst and sodium hydride (NaH) were purchased from Aldrich, Shanghai, China and used as received. Propargyl bromide, 1,5-cyclooctadiene (COD), *cis*-2-butene-1,4-diol, sodium azide (NaN_3) and sodium hydroxide (NaOH) were purchased from TCI Shanghai, China. Before use, COD and *cis*−2-butene-1,4-diol were distilled over calcium hydride (CaH_2) under reduced pressure. An alkynyl-capped poly (ethylene oxide) was synthesized via the reaction of poly(ethylene oxide) monomethyl ether (M_n = 2000 Da) with propargyl bromide in the presence of sodium hydride (NaH). All the organic solvents used in this work were obtained from Shanghai Reagent, China. Before use, chloroform and tetrahydrofuran (THF) were refluxed over sodium and then distilled.

Synthesis of 3-Bromopropylheptaphenyl POSS

3-Bromopropylheptaphenyl POSS was synthesized by following the method of literature reported by Fukuda et al.[37] with slight modification. First, phenyltrimethoxysilane [$C_6H_5Si(OMe)_3$] (32.020 g, 161.8 mmol), THF (195 mL), deionized water (3.760 g, 200.8 mmol) and sodium hydroxide (2.780 g, 69.5 mmol) were charged to a flask equipped with a magnetic stirrer and a condenser. After refluxed for 5 h, the system was cooled down to room temperature and then the reaction was performed for additional 20 h. All the solvents were removed via rotary evaporation to obtain the white solids. After dried at 40 °C *in vacuo* for 24 h, $Na_3O_{12}Si_7(C_6H_5)_7$ (32.260 g) was obtained with the yield of 98.5%. Second, the as-received $Na_3O_{12}Si_7(C_6H_5)_7$ was reacted with bromopropyltrichlorosilane to obtain 3-bromopropylheptaphenyl POSS via silylation reaction. Typically, $Na_3O_{12}Si_7(C_6H_5)_7$ (20.000 g, 21.1 mmol), triethylamine (2.93 mL, 21.1 mmol) and anhydrous THF (300 mL) were charged to a flask with vigorous stirring. Thereafter, 3-bromopropyltrichlorosilane (7.680 g, 25 mmol) was dropwise added at 0 °C. This reaction was carried out at 0 °C for 2 h and at room temperature for additional 24 h. Thereafter, the insoluble solids were filtered out and the reacted mixture was concentrated via rotary evaporation. The mixture was then dropped into a great amount of methanol to afford the precipitates. This dissolution–precipitation procedure was repeated three times to obtain the white solids. After dried in a vacuum oven at 30 °C for 24 h, 3-bromopropylheptaphenyl POSS (14.170 g) was obtained with the yield of 62.3%. ^{1}H NMR ($CDCl_3$, ppm): 0.96 (*m*, 2H, Si—C***H*****$_2$**—CH_2—CH_2—Br), 2.08 (*m*, 2H, Si—CH_2—C***H*****$_2$**—CH_2—Br), 3.42 (*m*, 2H, Si—CH_2—CH_2—C***H*****$_2$**—Br), 7.30–7.55, 7.70–7.87 (*m*, 35H, C_6***H*****$_5$**). ^{29}Si NMR ($CDCl_3$, ppm): −65.37, −77.76, −78.15.

Synthesis of 3-Azidopropylheptaphenyl POSS

3-Azidopropylheptaphenyl POSS was synthesized via the substitution reaction of 3-bromopropylheptaphenyl POSS with sodium azide (NaN_3). Typically, 3-bromopropylheptaphenyl POSS (3.000 g, 2.78 mmol) was added into a flask containing a magnetic stirrer. Thereafter, the mixture of THF (20 mL) with DMF (20 mL) and NaN_3 (0.190 g, 3.21 mmol) were added to the flask.This reaction was performed at room temperature for 24 h; the reacted mixture was concentrated and then dropped into a great amount of methanol to afford the precipitates. The precipitates were dried at 40 °C in a vacuum oven for 24 h and the product (2.320 g) was obtained with the yield of 78.1%. ^{1}H NMR ($CDCl_3$, ppm): 0.95 (*t*, 2H, Si—C***H*****$_2$**—CH_2—CH_2—N_3), 1.83 (*m*, 2H, Si—CH_2—C***H*****$_2$**—CH_2—N_3), 3.24 (*t*, 2H, Si—CH_2—CH_2—C***H*****$_2$**—N_3) and 7.29–7.54, 7.72–7.85 (*m*, 35H, C_6***H*****$_5$**).

Synthesis of 1,4-*Bis*(Prop-2-Ynyloxy)but-2-Ene

To a flask sodium hydride (4.800 g, 0.2 mol) and anhydrous THF (150 mL) were charged and then the solution of 2-butene-1,4-diol (2.200 g, 25 mmol) dissolved in 50 mL of anhydrous THF was slowly dropped into the flask at 0 °C. This reaction was performed at room temperature for 3 h and then propargyl bromide (8.900 g, 75 mmol) dissolved in 15 mL of anhydrous THF was dropwise added. The reaction

was carried out at room temperature for additional 24 h. The insoluble solids were removed via filtration and the solvent was removed via rotary evaporation. The product was purified by passing through a silica gel column with the mixture of ethyl acetate and petroleum ether (1:5 vol) as the eluent. The product (9.580 g) was obtained with a yield of 91.5%. ^{1}H NMR (ppm, $CDCl_3$): 2.41 (*t*, 2H, ***H***C≡CCH$_2$), 4.01 (*m*, 4H, CHC***H$_2$***OCH$_2$), 4.09 (*d*, 4H, HC≡CC***H$_2$***), 5.70, 577 (*d*, CH$_2$C***H***=C*H*CH$_2$).

Synthesis of 1,4-DiPOSS-but-2-Ene

1,4-DiPOSS-but-2-ene (denoted POSS-CTA) was synthesized by the copper-catalyzed Huisgen cycloaddition reaction (i.e., click chemistry) between 3-azidopropylheptaphenyl POSS and 1,4-*bis* (prop-2-ynyloxy)but-2-ene. Typically, 3-azidopropylheptaphenyl POSS (2.410 g, 2.5 mmol), 1,4-*bis*(prop-2-ynyloxy) but-2-ene (0.164 g, 1 mmol) and tetrahydrofuran (30 mL) were charged to a flask equipped with a magnetic stirrer. The system was purged with highly pure nitrogen for 45 min and then Cu(I)Br (4.0 mg) and PMDETA (10.2 μL) were added. The reaction was carried out at room temperature for 24 h. Thereafter, an alkynyl-capped poly(ethylene oxide) monomethyl ether (M_n = 2000 Da) (1.500 g, 0.75 mmol with respect of alkynyl group) was added to the flask with vigorous stirring. The reaction was carried out for additional 24 h. The reacted mixture was dropwise added to 200 mL of deionized water with vigorous stirring. At room temperature, the system was maintained with vigorous stirring for 2 h. After standing for 30 min, the insoluble portion was isolated. After drying *in vacuo* at room temperature for 12 h, the product (2.120 g) was obtained with the yield of 76%. ^{1}H NMR (ppm, $CDCl_3$): 0.83 (*m*, 4H, SiC***H$_2$***CH$_2$CH$_2$-trizole), 1.28 (*m*, 4H, SiC***H$_2$***CH$_2$CH$_2$-triazole), 4.01 (*m*, 4H, CHC***H$_2$***OCH$_2$), 4.09 (*d*, 4H, HC≡CC***H$_2$***), 4.27 (*m*, 4H, SiCH$_2$CH$_2$C***H$_2$***-trizole), 4.53 (*d*, 4H, triazole—C***H$_2$***—O), 5.85 (m, 2H, CH$_2$C***H***=C***H***CH$_2$), 7.31–7.81 (*m*, 70 H, protons of aromatic ring of POSS).

Synthesis of POSS-Terminated PCOD Telechelics

By using Grubbs second catalyst, the ring-opening metathesis polymerization (ROMP) of cyclooctadiene (COD) was performed to afford the POSS-terminated PCOD telechelics. Typically, to a predried flask POSS-CTA (0.054 g, 0.022 mmol) and anhydrous chloroform (10 mL) were charged and the solution was purged with nitrogen for 30 min. Thereafter, Grubbs second generation catalyst (2.2 mg, 2.6 mmol) dissolved in 1.0 mL of chloroform was added. The flask was immersed in a thermostated bath at 40 °C and then COD (0.300 g, 2.78 mmol) was added. The polymerization was performed at 40 °C for 10 h with vigorous stirring. The polymerization was terminated by adding the mixture of methanol (50 mL) with 1.0M hydrochloric acid (8 mL). The solution was concentrated via rotary evaporation and then precipitated in methanol. After dried in vacuum at 30 °C for 24 h, the resulting product (0.340 g) was obtained with the yield of 96.0%. ^{1}H NMR (ppm, $CDCl_3$): 0.83 (*m*, 4H, SiC***H$_2$***CH$_2$CH$_2$—trizole), 1.28 (*m*, 4H, SiC***H$_2$***CH$_2$CH$_2$-triazole), 2.06 (*d*, 992H, C***H$_2$***CH=CHC***H$_2$***C***H$_2$***CH=CHC***H$_2$***), 4.01 (*m*, 4H, CHC***H$_2$***OCH$_2$), 4.09 (*d*, 4H, HC≡CC***H$_2$***), 4.27 (*m*, 4H, SiCH$_2$CH$_2$C***H$_2$***—trizole), 4.53 (*d*, 4H, triazole—C***H$_2$***—O), 5.39 (*d*, 496H, CH$_2$C***H***=C***H***CH$_2$CH$_2$C***H***=C***H***CH$_2$), 5.85 (*m*, 2H, OCH$_2$C***H***=C***H***CH$_2$O), 7.31–7.81 (*m*, 70 H, protons of aromatic ring of POSS). GPC: M_n = 18,300 Da with M_w/M_n = 1.62.

Measurements and Techniques

Nuclear Magnetic Resonance (NMR) Spectroscopy

The ^{1}H NMR measurement was performed on an Avance III HD 400 MHz NMR spectrometer (Bruker BioSpin, Germany) at room temperature. Deuterium chloroform ($CDCl_3$) was used as the solvent with tetramethylsilane (TMS) as an internal reference.

Gel Permeation Chromatography (GPC)

The molecular weights and molecular weight distribution were determined on a Waters 717 Plus autosampler gel permeation chromatography apparatus equipped with Waters RH columns and a Dawn Eos multiangle laser light scattering detector (Wyatt Technology Corp., USA). The GPC measurements were performed at room temperature with THF as the eluent at the rate of 1.0 mL × min^{-1}. The molecular weights were expressed relative to polystyrene standards.

Atomic Force Microscopy (AFM)

For the preparation of AFM specimens, all the POSS-capped PCOD telechelics were dissolved in THF at the concentration of 5 wt % and the solutions were spin-coated onto silicon wafers. The solvent was evaporated at room temperature for 4 h and the residual solvent was eliminated *in vacuo* at 40 °C for 4 h; the thickness of the films was controlled to be at least 25 μm. The morphological observation was carried out on a CSPM 5500 atomic force microscopy (Benyuan Nano-instruments, China) in tapping mode. A tip fabricated from silicon (125 μm in length with ca. 300 kHz resonant frequency) was used for scanning and the scanning rate was 2.0 Hz.

Differential Scanning Calorimetry (DSC)

The calorimetric measurements were performed on a DSC8000 differential scanning calorimeter (Perkin Elmer, USA) in a dry nitrogen atmosphere. The samples were first heated up to 150 °C and held at this temperature for 3 min to erase the thermal history, followed by quenching to −60 °C. After that, the samples were scanned to 120 °C at the heating rate of 20 °C × min^{-1} and cooled down to −60 °C at the rate of −10 °C × min^{-1} to record the thermograms. Melting temperatures (T_ms) and crystallization temperatures (T_cs) were taken as the temperatures at the maxima of endothermic transitions and the minima of exothermic transitions, respectively.

Wide Angle X-Ray Diffraction

The wide-angle X-ray diffraction (XRD) experiments were carried out on a D8 Advance X-ray diffractometer (Bruker Corp., Germany) with CuKα (λ = 0.154 nm) with irradiation at 40 kV and 30 mA using a Ni filter. Data were recorded in the range of 2θ = 5–50° at the scanning rate and step size of 2.0° × min^{-1} and 0.02°, respectively.

Thermogravimetric Analysis (TGA)

Thermal stability of plain PCOD and the POSS-terminated PCOD telechelics was investigated with a Q5000 thermal

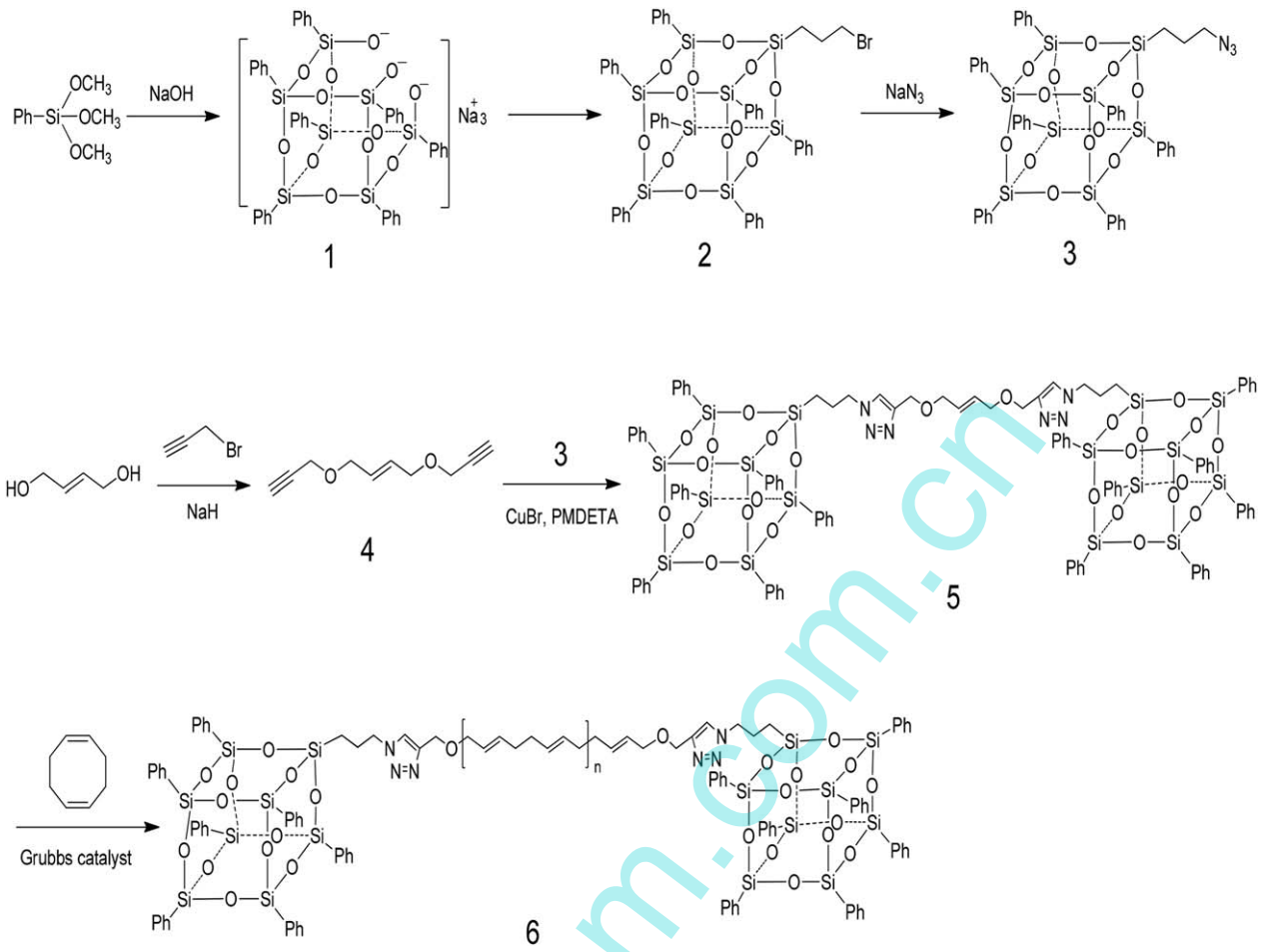

SCHEME 1 Synthesis of POSS-terminated PCOD telechelics.

gravimetric analyzer (TA Instruments, USA). The measurements were conducted in nitrogen atmosphere from 40 to 800 °C at a heating rate of 20 °C × min^{-1}.

Static Contact Angle Analysis

Plain PCOD and the POSS-terminated PCOD telechelics were dissolved in chloroform (10.0 mg/mL) and the solutions were cast onto glass slides. The majority of solvent was evaporated at room temperature for 4 h and the residual solvent was eliminated in a vacuum over at 30 °C for 2 h. The films with free surfaces and with the thickness of 25 μm and were subjected to the measurement of static contact angles on a DSA30 contact angle measurement apparatus (Krüss GmbH, Germany). Ultrapure water and ethylene glycol were used as the probe liquids, respectively.

RESULTS AND DISCUSSION

Synthesis of POSS-Terminated PCOD Telechelics

The route of synthesis for α,ω-diPOSS-terminated PCOD telechelics was shown in Schemes 1 and 2. With 1,4-diPOSS-but-2-ene as the chain transfer agent (denoted POSS-CTA), the ring-opening metathesis polymerization of cyclooctadiene (COD) was carried out in the presence of Grubbs second catalyst. To obtain POSS-CTA, 1,4-bis(prop-2-ynyloxy)but-2-ene was first synthesized via the reaction of *cis*−2-butene-1,4-diol with propargyl bromide in the presence of sodium hydride (NaH). For the synthesis of 3-azidopropylheptaphenyl POSS, phenyltrimethoxysilane was first hydrolyzed and rearranged into heptaphenyltricycloheptasiloxane trisodium silanolate [$Na_3O_{12}Si_7(C_6H_5)_7$]; thereafter, the silylation reaction between $Na_3O_{12}Si_7(C_6H_5)_7$ and 3-bromopropyltrichlorosilane was carried out to afford 3-bromopropylheptaphenyl POSS.[38–40] The bromine atom of 3-bromopropylheptaphenyl POSS was then substituted with azido group through its reaction with sodium azide (NaN_3). Shown in Figure 1 are the ^{1}H NMR spectra of 1,4-bis(prop-2-ynyloxy)but-2-ene and 3-azidopropylheptaphenyl POSS. For 1,4-bis(prop-2-ynyloxy)but-2-ene, the signals of resonance at 2.42, 4.75, 4.92, and 5.85 ppm are assignable to the protons of alkynyl, methylene groups connected to oxygen atom and methine in 2-butene moiety, respectively. For 3-azidopropylheptaphenyl POSS, the signals of resonance at 0.83, 1.67, 3.25, and 7.1–7.8 ppm are assignable to the protons of the methylene connected to a vertex silicon atom of POSS, the second methylene in 3-azidopropyl groups and the methylene connected to triazole ring and phenyl groups of POSS, respectively. The ^{1}H NMR spectroscopy

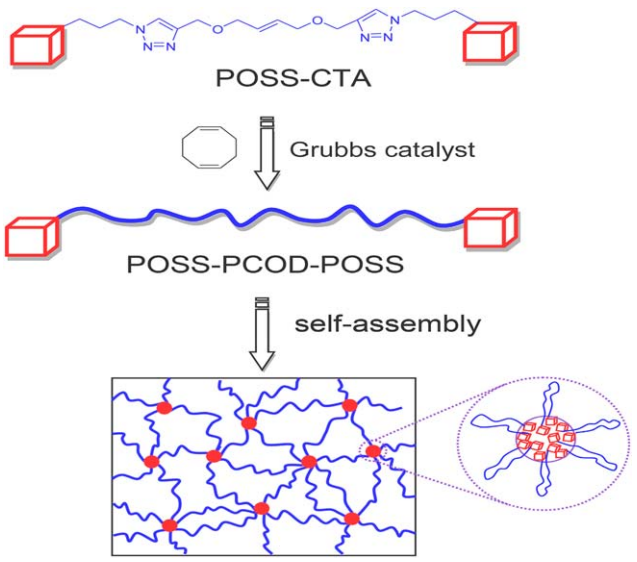

SCHEME 2 Synthesis and self-assembly behavior of POSS-terminated PCOD telechelics. [Color figure can be viewed at wileyonlinelibrary.com]

indicates that both 1,4-bis(prop-2-ynyloxy)but-2-ene and 3-azidopropylheptaphenyl POSS have been successfully synthesized. Both of the compounds were employed to synthesize 1,4-diPOSS-but-2-ene via the copper-catalyzed cycloaddition reaction (viz. click chemistry). To ensure the complete reaction of all alkynyl groups of 1,4-*bis*(prop-2-ynyloxy)but-2-ene with azido groups, 3-azidopropylheptaphenyl POSS was controlled to be excess by 25 mol %. The excess 3-azidopropylheptaphenyl POSS was allows to react with an alkynyl-capped poly(ethylene oxide) (M_n = 2000 Da) to form POSS-capped poly(ethylene oxide). To

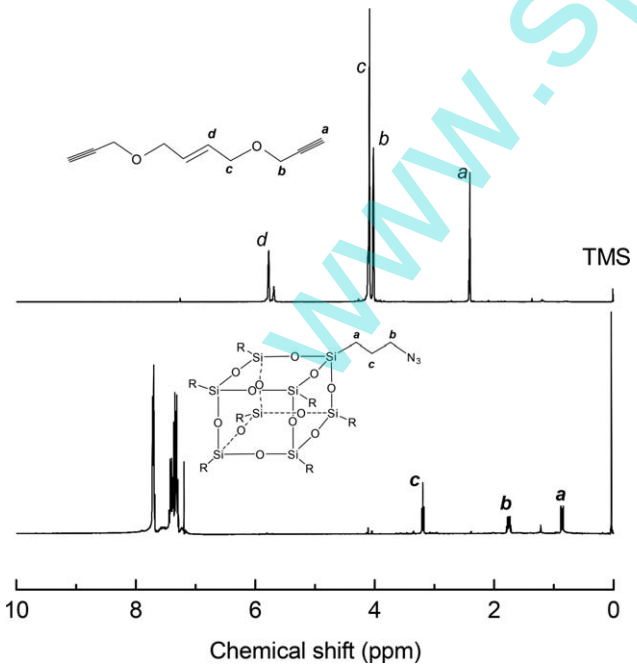

FIGURE 1 ^{1}H NMR spectra of 1,4-*bis*(prop-2-ynyloxy)but-2-ene and 3-azido propyl heptaphenyl POSS.

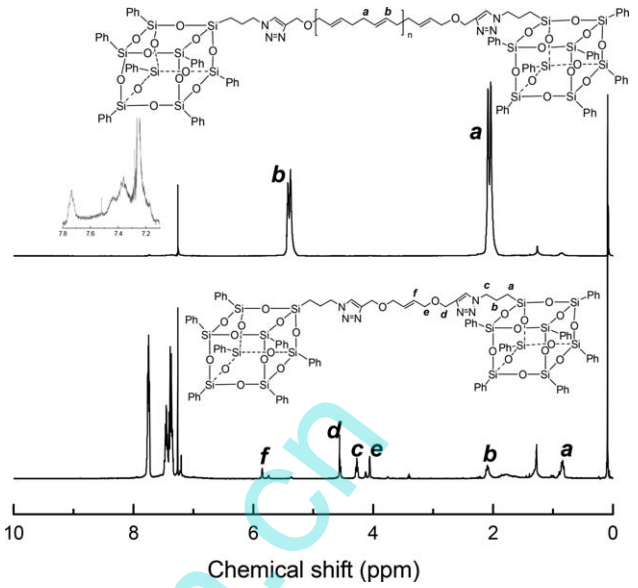

FIGURE 2 ^{1}H NMR spectra of POSS-CTA and POSS-PCOD16K-POSS.

remove the POSS-capped poly(ethylene oxide), the reacted mixture was dropped into deionized water. In this case, 1,4-diPOSS-but-2-ene (*viz.* POSS-CTA) remained insoluble in water whereas the POSS-capped poly(ethylene oxide) was dispersed in the form of micelles in water. The difference insolubility allowed the isolation and purification of 1,4-diPOSS-but-2-ene. Shown in Figure 2 is the ^{1}H NMR spectrum of POSS-CTA. This spectrum combined the signals of resonance from 1,4-*bis*(prop-2-ynyloxy) but-2-ene and 3-azidopropylheptaphenyl POSS; no signal of the resonance at 2.42 ppm attributable to protons of alkynyl groups was detected. The ^{1}H NMR spectroscopy indicates that the click reaction has been performed to completion. According to the ratio of integral intensity of the protons of methine groups in 2-butene moiety to methylene protons adjacent to POSS cages, it was judged that the POSS-CTA was successfully obtained.

With the above POSS-CTA as the chain transfer agent, the ring-opening metathesis polymerization (ROMP) of cyclooctadiene was carried out by the use of Grubbs second generation catalyst. By controlling the mass ratio of POSS-CTA to cyclooctadiene monomer, a series of POSS-terminated polycyclooctadiene telechelics (denoted POSS-PCOD-POSS) with variable lengths of PCOD were obtained (see Table 1). Also shown in Figure 2 is the ^{1}H NMR spectrum of POSS-

TABLE 1 Results of ROMP Polymerization for COD in the Presence of POSS-CTA

Samples	M_n (Da)	L_{PCOD} (Da)	M_w/M_n
POSS-PCOD4K-POSS	6,400	4,155	1.63
POSS-PCOD10K-POSS	12,200	9,955	1.61
POSS-PCOD14K-POSS	15,900	13,655	1.57
POSS-PCOD16K-POSS	18,300	16,055	1.62
POSS-PCOD21K-POSS	23,200	20,955	1.78

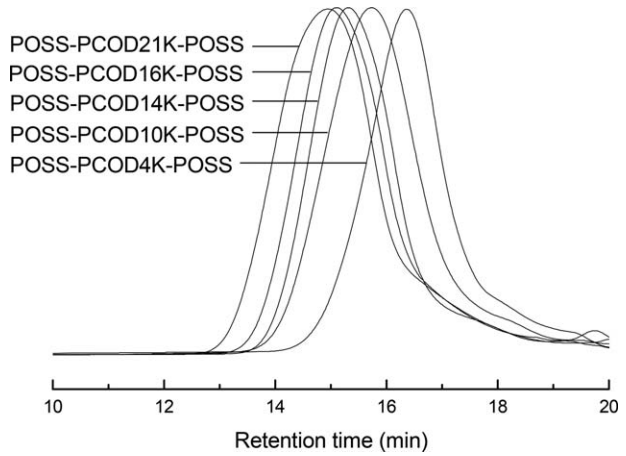

FIGURE 3 GPC curves of POSS-terminated PCOD telechelics.

PCOD16K-POSS. The signals of resonance in the range of 7.3 and 7.9 ppm are assignable to the protons of phenyl group of POSS cages; the signals of resonance at 2.06 and 5.39 ppm are assigned to the protons of methylene and carbon-carbon double bonds in the main chains of PCOD, respectively. The ^{1}H NMR spectroscopy indicates that the products combined the structural features from POSS and PCOD. All the POSS-terminated PCOD telechelics were subjected to gel permeation chromatography (GPC) to measure their molecular weights. The GPC profiles are presented in Figure 3 and the results of the molecular weights are summarized in Table 1. Notably, all the GPC curves displayed unimodal distribution of molecular weights and no POSS-CTA was detected in the resulting polymers. The values of polydispersity index (PDI) were measured to be in the range of 1.57–1.78, which were comparable to the values reported in literature with other chain transfer agents for ROMP of COD.[23,41–56] The GPC results indicate that the 1,4-diPOSS-but-2-ene has been successfully employed as the chain transfer agent for the ROMP of COD and that the POSS-terminated PCOD telechelics were successfully obtained.

Morphologies of POSS-Terminated PCOD Telechelics

The morphologies of POSS-terminated PCOD telechelics were investigated by means of atomic force microscopy (AFM). The films of the samples were prepared via spin-coating technique. The surface AFM micrographs are presented in Figure 4. The left and right images are the height and phase shift images, respectively. It is seen that all the POSS-terminated PCOD telechelics displayed microphase-separated morphologies. The formation of the microphase separation is attributable to the immiscibility of the POSS with PCOD. In terms of the volume fraction of POSS and the difference in viscoelastic properties between POSS and PCOD, it is judged that the dark regions are assignable to PCOD matrix while the light are attributed to the POSS domains. It is seen that POSS-PCOD4K-POSS displayed a co-continuous morphology. With increasing the length of the midchain (viz. PCOD), the continuous POSS microphase was gradually transformed into the isolated (or dispersed) microdomains, that is, a

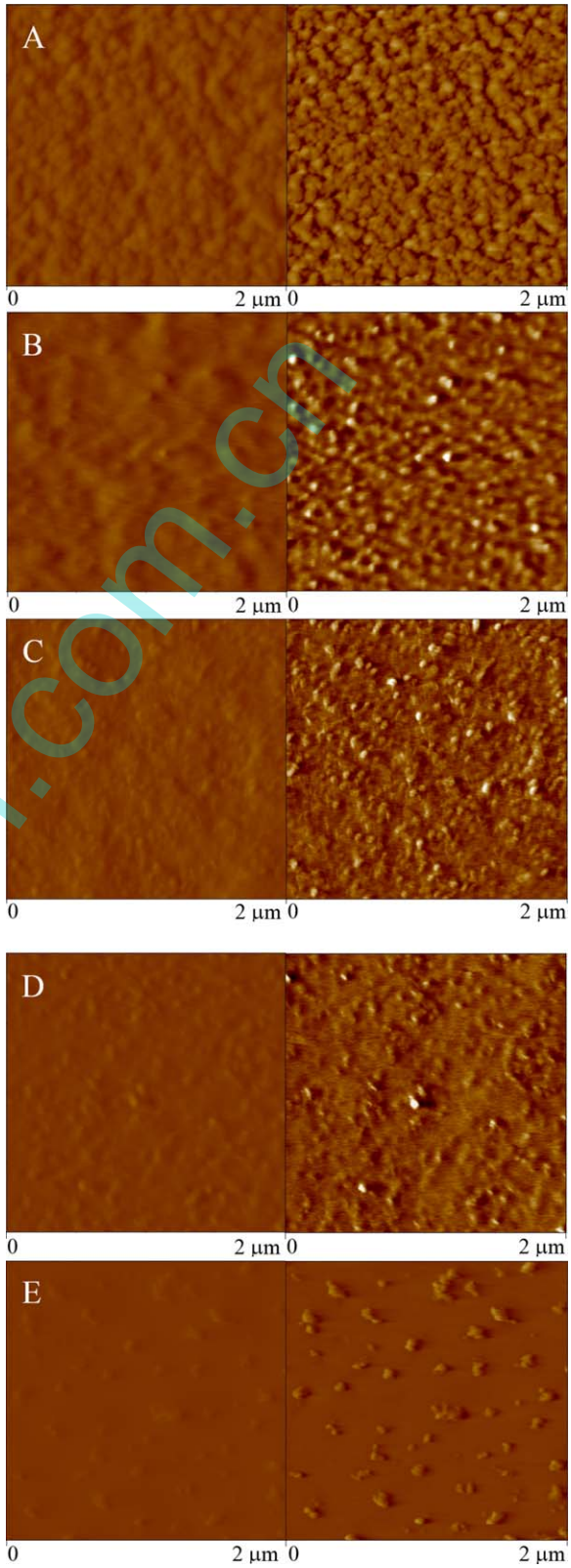

FIGURE 4 AFM micrographs of POSS-terminated PCOD telechelics. [Color figure can be viewed at wileyonlinelibrary.com]

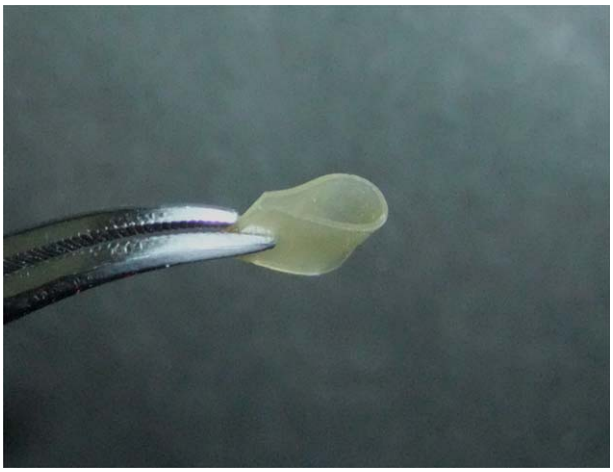

FIGURE 5 The photo of POSS-PCOD16K-POSS. [Color figure can be viewed at wileyonlinelibrary.com]

morphological transition occurred [see Fig. 4(B−E)]. For POSS-PCOD16K-POSS and POSS-PCOD21K-POSS, the spherical POSS microdomains with the size of 30–50 nm in diameter appeared and were dispersed in the continuous PCOD matrices. It should be pointed that the sizes of the POSS microdomains revealed in the AFM micrographs could exceed those in bulks. Owing to the low surface energy for the organosilicon-containing component, the POSS end groups would be enriched to the interface between the sample and air. Nonetheless, the AFM results indicate that the organic−inorganic PCOD telechelics were microphase-separated and their morphologies were quite dependent on the lengths of PCOD midchains.

The AFM results remind that the POSS microdomains would behave as the physical crosslinking sites of PCOD chains. As a consequence, the POSS-terminated PCOD telechelics would exhibit the properties of crosslinked elastomers, depending on the lengths of PCOD midchains. Representatively shown in Figure 5 is a photo of POSS-PCOD16K-POSS at room temperature. The homogenous and transparent sample displayed the rubber-like feature with good dimensional stability, in marked contrast to the PCOD homopolymer with the identical molecular weight, which was just a viscous liquid.

Surface Properties of POSS-Terminated PCOD Telechelics

Owing to the lower surface free energy, the POSS groups would be migrated onto the surface of the POSS-terminated PCOD telechelics. The enrichment of POSS portion will significantly affect the surface hydrophobicity of the samples, which was readily investigated by the measurements of static surface contact angles and surface free energies.[57,58] In this work, the static surface contact angles were measured with water and ethylene glycol as probe liquids, respectively. Shown in Figure 6 are the plots of the water contact angles of the POSS-terminated PCOD telechelics. For the plain PCOD, the water contact angle was measured to be 102.7°. Upon introducing POSS at the ends of PCOD chains, the water contact angles were significantly increased; the water contact angles increased with increasing the content of POSS or with decreasing the length of PCOD midchains. For POSS-PCOD21K-POSS, the water contact angle was enhanced up to 121.1°. The increased contact angles indicate that the surface hydrophobicity of the samples was significantly enhanced. In terms of the values of contact angles with water and ethylene glycol as the probe liquids, the surface free energies of the POSS-terminated PCOD telechelics were calculated with the geometric mean model[59–61]:

$$\cos\theta = \frac{2}{r_L}\left[\left(r_L^d r_s^d\right)^{\frac{1}{2}} + \left(r_L^p r_s^p\right)^{\frac{1}{2}}\right] - 1 \quad (1)$$

$$r_s = r_s^d + r_s^p \quad (2)$$

where θ is the contact angle and γ_L is the liquid surface tension; r_s^d and r_s^p are the dispersive and polar components of γ_L, respectively. It was found that the surface free energy was decreased from 17.18 to 11.31 mN/m while the content of POSS increased from 0 to 35.1 wt % (see Table 2). The values of the polar component was quite sensitive to the content of POSS, indicating that the incorporation of POSS altered the distribution of the polar groups on the surface energy of materials, that is, the POSS microdomains were migrated onto the surface screened the PCOD chains to some extent (see Fig. 4). As a consequence, the surface free energy of POSS-terminated PCOD telechelics was significantly decreased.

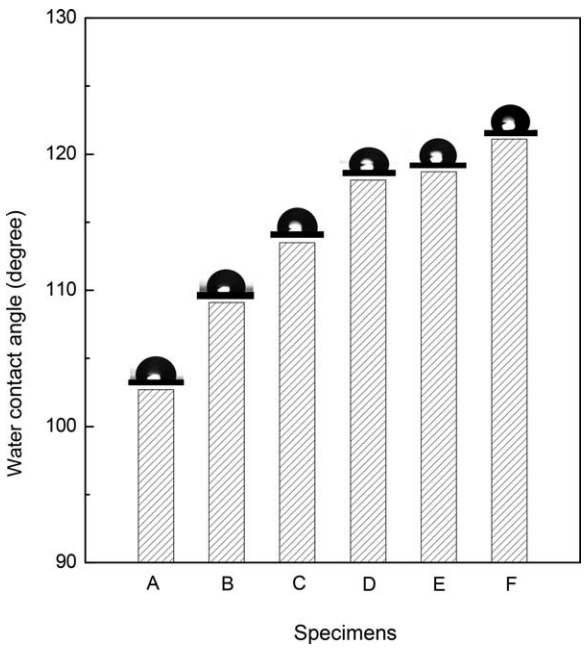

FIGURE 6 Plots of water contact angles for plain PCOD and POSS-terminated PCOD telechelics at room temperature: (A) PCOD (M_n = 48,200 Da with M_w/M_n = 2.1); (B) POSS-PCOD21K-POSS; (C) POSS-PCOD16K-POSS; (D) POSS-PCOD14K-POSS; (E) POSS-PCOD10K-POSS; (F) POSS-PCOD4K-POSS.

TABLE 2 Static Contact Angles and Surface Free Energy of Pure PCOD and the POSS-Terminated PCOD Telechelics

	Static Contact Angle		Surface Free Energy (mN/m)		
Samples	θ_{water}	$\theta_{ethylene\ glycol}$	γ^d_s	γ^p_s	γ_s
PCOD (M_n = 48,200 Da with M_w/M_n = 2.1)	102.7 ± 0.08	82.5 ± 0.36	15.13	2.05	17.18
POSS-PCOD4K-POSS	109.1 ± 0.21	89.8 ± 0.16	13.13	1.12	14.25
POSS-PCOD10K-POSS	113.5 ± 0.16	92.1 ± 0.08	12.16	0.61	12.77
POSS-PCOD14K-POSS	118.1 ± 0.13	96.6 ± 0.24	11.74	0.25	11.99
POSS-PCOD16K-POSS	118.7 ± 0.24	99.2 ± 0.12	11.63	0.18	11.81
POSS-PCOD21K-POSS	121.1 ± 0.18	101.5 ± 0.20	11.24	0.07	11.31

Water: γ_L = 72.8 mN/m, γ^d_L = 21.8 mN/m, γ^p_L = 51.0 mN/m. Ethylene glycol: γ_L = 48.3 mN/m, γ^d_L = 29.3 mN/m, γ^p_L = 19.0 mN/m.

Thermal Properties of POSS-Terminated PCOD Telechelics

The plain PCOD and the POSS-terminated PCOD telechelics were subjected to differential scanning calorimetry (DSC). All the samples were first heated up to 120 °C and held at this temperature for 3 min to erase the thermal history and then the heating scans were recorded at the heating rate of 20 °C/min. Thereafter, the cooling scans were recorded at the rate of −10 °C/min. The DSC curves of the plain PCOD (M_n =48,200 Da with M_w/M_n = 2.1) and the POSS-terminated PCOD telechelics are shown in Figure 6. For the plain PCOD, no detectable thermal transition was found in the range of temperature from −60 to 120 °C. It should be pointed out that the glass transition temperature of PCOD was reported to be as low as −95 °C,[62] which was beyond the temperature range of the DSC measurements with the built-in intracooler accessory. The observation that neither exothermic nor endothermic transition attributable to crystallization or melting of the PCOD crystals was exhibited suggests that the rate of crystallization was too slow to be detected under the present condition although PCOD was reported to be crystallizable.[62] In marked contrasted to the plain PCOD, the POSS-terminated PCOD telechelics displayed the endothermic peaks in the heating scans and the exothermic peaks in the cooling scans, respectively. These exothermic and endothermic peaks are attributable to the crystallization and melting of the samples under the conditions of DSC scans. For POSS-PCOD4K-POSS, a broad endothermic peak appeared at about 4 °C; it is attributable to the melting transition of PCOD. While the length of PCOD was more than 10,000 Da, the melting transitions became increasingly pronounced; the intensities of the melting peaks increased with increasing the lengths of PCOD midchains. In all the cases, the exothermic peaks were also displayed in the cooling thermograms of the POSS-terminated PCOD telechelics (see Fig. 7). The exothermic peaks are attributable to the crystallization behavior of PCOD in the cooling scans. The DSC results indicate that the terminal POSS ends facilitate the crystallization of PCOD. It is proposed that the POSS microdomains could act as the heterogeneous nucleating agent to accelerate the crystallization of PCOD. Notably, the melting temperatures (T_m's) of PCOD did not monotonously increased with increasing the fraction of POSS in the organic−inorganic telechelics. Both POSS-PCOD16K-POSS and POSS-PCOD14K-POSS displayed the maximum melting temperatures (T_ms) at 20 °C. Thereafter, the T_m's decreased with increasing the fraction of POSS in the organic–inorganic telechelics. For POSS-PCOD10K-POSS and POSS-PCOD4K-POSS, the T_m's were depressed to 17 and 3 °C, respectively. In the meantime, the values of melting and crystallization enthalpy were also significantly decreased. It is proposed that the POSS microdomains had two opposite trends to affect the crystallization of PCOD. On the one hand, the POSS microdomains acted as the heterogeneous nucleating agent to promote the crystallization of PCOD chains. This effect is

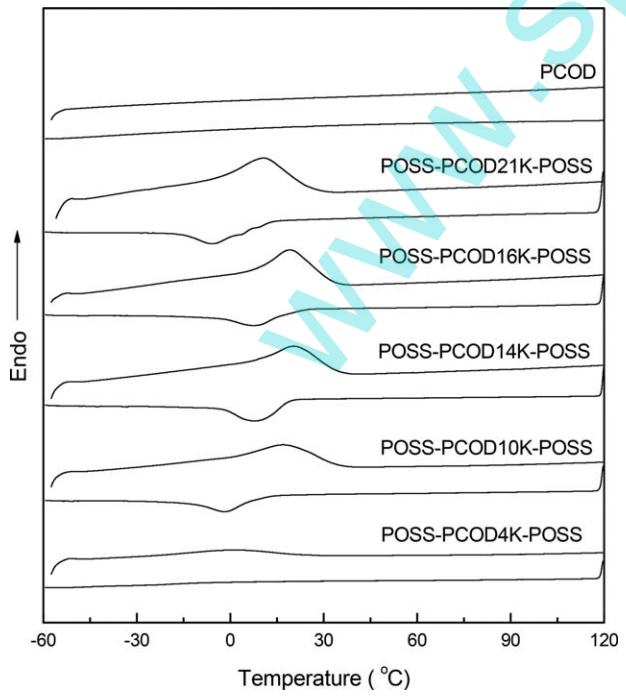

FIGURE 7 DSC curves of POSS-terminated PCOD telechelics.

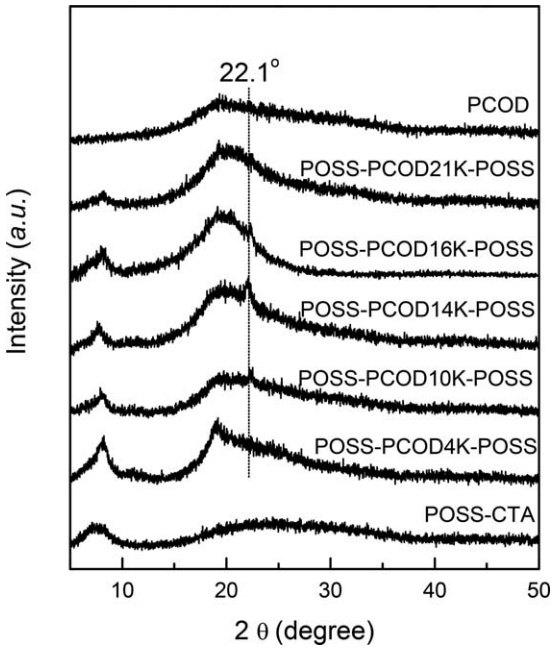

FIGURE 8 XRD curves of POSS-terminated PCOD telechelics.

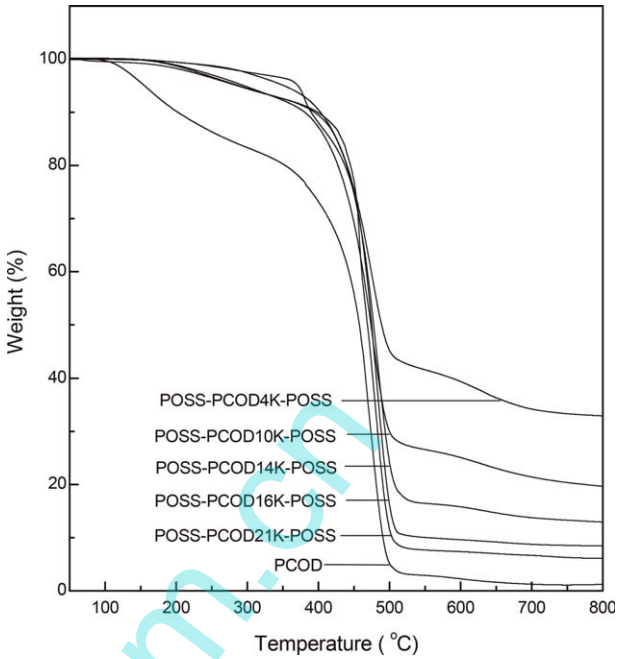

FIGURE 9 TGA curves of Plain PCOD and POSS-terminated PCOD telechelics.

pronounced for the samples in which the fraction of POSS in the organic–inorganic telechelics was not very high (e.g., POSS-PCOD21K-POSS, POSS-PCOD16K-POSS and POSS-PCOD14K-POSS). On the other hand, the POSS microdomains could exert the restriction on the crystallization owing the nanoreinforcement of the POSS microdomains on PCOD matrix. This effect was dominant while the fraction of POSS in the organic–inorganic telechelics was sufficiently high (e.g., POSS-PCOD10K-POSS and POSS-PCOD4K-POSS).

The crystallization behavior of the POSS-terminated PCOD telechelics can be further confirmed with wide-angle X-ray diffraction (XRD) measurements. Shown in Figure 8 are the XRD curves of POSS-CTA, the plain PCOD and the POSS-terminated PCOD telechelics. For POSS-CTA, a diffraction peak at $2\theta = 8.15°$ was displayed; this peak was found in all the POSS-terminated PCOD telechelics. This peak was ascribed to the aggregates of POSS cages.[63] For the plain PCOD, only a broad amorphous halo at $2\theta = 19.28°$ was displayed, suggesting that this sample was amorphous. In marked contrast to the plain PCOD, there appeared the sharp diffraction peak at $2\theta = 22.1°$ for all the POSS-terminated PCOD telechelics besides the broad halo and the diffraction peak from POSS microdomains. From the viewpoint of chain structures, PCOD can be taken as *trans*−1,4-polybutadiene. It is plausible to propose that the diffraction peak at 22.1° for POSS-terminated PCOD telechelics is attributable to the reflections as in *trans*−1,4-polybutadiene crystals, that is, this diffraction peak resulted from the (100) reflection with *pseudo*-hexagonal lattice with the cell parameter of $a = b = 4.54$ Å, $c = 4.85$ Å.[64,65] It is seen that the intensity of the sharp diffraction peak increased with increasing the length of PCOD in the POSS-terminated PCOD telechelics. While the length of PCOD increased to 21,000 Da, the intensity decreased slightly, indicating the crystallinity of the samples decreased. This observation was in accord with the DSC (see Fig. 7).

Shown in Figure 9 were TGA curves of the plain PCOD and the POSS-terminated PCOD telechelics recorded in nitrogen atmosphere at 20 °C/min. For the plain PCOD, the initial degradation temperature (T_d's) was detected to be about 156 °C. Notably, the POSS-terminated PCOD telechelics displayed the T_d's much higher than that of the plain PCOD. The rates of the thermal degradation of the organic−inorganic telechelics were much lower than that of the plain PCOD. This observation suggests that the incorporation of POSS at the ends of PCOD chains retarded the random-chain scission. In addition, all the POSS-terminated PCOD telechelics exhibited the residues of degradation at 710 °C and the yields of degradation residues increased with increasing the contents of POSS in the organic–inorganic telechelics. In terms of the initial degradation temperatures (T_d's) and the yields of residue, it is judged that the POSS-terminated PCOD telechelics displayed the improved the thermal stability compared to plain PCOD.

CONCLUSIONS

With an end-group-first approach, POSS-terminated polycyclooctadiene (PCOD) telechelic polymers were successfully synthesized via ring-opening metathesis polymerization (ROMP) with 1,4-diPOSS-but-2-ene (POSS-CTA) as the chain transfer agent. By controlling the molar ratios of POSS-CTA to cyclooctadiene, POSS-terminated PCOD telechelics with variable lengths of PCOD were obtained. Atomic force microscopy (AFM) showed that all the POSS-terminated PCOD telechelics were microphase-separated, in which the

spherical POSS aggregates with the size of 20–50 nm in diameter were dispersed in continuous PCOD matrix via POSS–POSS interactions. In the POSS-terminated PCOD telechelics, inorganic POSS molecules acted as the heterogeneous nucleating agent to accelerate the crystallization of PCOD. The static contact angle measurements indicated that the POSS-terminated PCOD telechelics displayed a significant enhancement in surface hydrophobicity as well as reduction in surface free energy. The improvement in surface properties was ascribed to the enrichment of POSS moiety on the surface of the materials.

ACKNOWLEGMENTS

The financial supports from Natural Science Foundation of China (No. 21304058, 51133003 and 21274091) are gratefully acknowledged. One of the authors (CZ) would like to thank Shanghai Natural Science Foundation for the partial support under the project (No. 15ZR1421300).

REFERENCES AND NOTES

1 J. J. Schwab, J. D. Lichtenhan, *Appl. Organomet. Chem.* **1998**, *12*, 707–713.

2 G. Li, L. Wang, H. Ni, C. U. Pittman. Jr., *J. Inorg. Org. Polym.* **2001**, *11*, 123–154.

3 Y. Abe, T. Gunji, *Prog. Polym. Sci.* **2004**, *29*, 149–182.

4 K. Zeng, Y. Fang, S. Zheng, *J. Polym. Sci. Part B: Polym. Phys.* **2009**, *47*, 504–516.

5 B. S. Kim, P. T. Mather, *Macromolecules* **2002**, *35*, 8378–8384.

6 L. Wang, C. Zhang, S. Zheng, *J. Mater. Chem.* **2011**, *21*, 19344–19352.

7 K. Wei, L. Wang, S. Zheng, *Polym. Chem.* **2013**, *4*, 1491–1501.

8 J. Choi, J. Harcup, A. F. Yee, Q. Zhu, R. M. Laine, *J. Am. Chem. Soc.* **2001**, *123*, 11420–11429.

9 D. Neumann, M. Fisher, L. Tran, J. G. Matisons, *J. Am. Chem. Soc.* **2002**, *124*, 13998–13405.

10 K. Zeng, L. Wang, S. Zheng, *J. Phys. Chem.* **2009**, *113*, 11831–11840.

11 J. Normatov, M. S. Silverstein, *Macromolecules* **2007**, *40*, 8329–8335.

12 S. S. Chhatre, J. O. Guardado, B. M. Moore, T. S. Haddad, J. M. Mabry, G. H. McKinley, R. E. Cohen, *ACS Appl. Mater. Interfaces* **2010**, *2*, 3544–3554.

13 J. Wei, B. Tan, Y. Bai, J. Ma, X. Lu, *J. Phys. Chem. B* **2011**, *115*, 1929–1935.

14 K. Zeng, S. Zheng, *J. Phys. Chem.* **2009**, *210*, 783–791.

15 B. S. Kim, P. T. Mather, *Macromolecules* **2006**, *39*, 9253–9260.

16 W. Zhang, A. H. E. Mueller, *Macromolecules* **2010**, *43*, 3148–3152.

17 L. Wang, K. Zeng, S. Zheng, *ACS Appl. Mater. Interfaces* **2011**, *3*, 898–909.

18 C. Fraser, R. H. Grubbs, *Macromolecules* **1995**, *28*, 7248–7255.

19 M. A. Hillmyer, S. T. Nguyen, R. H. Grubbs, *Macromolecules* **1997**, *30*, 718–721.

20 M. K. Mahanthappa, F. S. Bates, M. A. Hillmyer, *Macromolecules* **2005**, *38*, 7890–7894.

21 L. M. Pitet, B. M. Chamberlain, A. W. Hauser, M. A. Hillmyer, *Macromolecules* **2010**, *43*, 8018–8025.

22 L. M. Pitet, M. A. Hillmyer, *Macromolecules* **2011**, *44*, 2378–2381.

23 C. W. Bielawski, R. H. Grubbs, *Prog. Polym. Sci.* **2007**, *32*, 1–29.

24 C. Cheng, E. Khoshdel, K. L. Wooley, *Macromolecules* **2007**, *40*, 2289–2292.

25 S. Rajaram, T. L. Choi, M. Rolandi, J. M. J. Fréchet, *J. Am. Chem. Soc.* **2007**, *129*, 9619–9621.

26 M. J. Allen, K. Wangkanont, R. T. Raines, L. L. Kiessling, *Macromolecules* **2009**, *42*, 4023–4027.

27 Y. Xia, J. A. Kornfield, R. H. Grubbs, *Macromolecules* **2009**, *42*, 3761–3766.

28 Z. Li, J. Ma, N. S. Lee, K. L. Wooley, *J. Am. Chem. Soc.* **2011**, *133*, 1228–1231.

29 K. Zhang, M. A. Lackey, J. Cui, G. N. Tew, *J. Am. Chem. Soc.* **2011**, *133*, 4140–4148.

30 J. A. Johnson, Y. Y. Lu, A. O. Burts, Y. H. Lim, M. G. Finn, J. T. Koberstein, N. J. Turro, D. A. Tirrell, R. H. Grubbs, *J. Am. Chem. Soc.* **2011**, *133*, 559–566.

31 N. Leventis, C. Sotiriou-Leventis, D. P. Mohite, Z. J. Larimore, J. T. Mang, G. Churu, H. Lu, *Chem. Mater.* **2011**, *23*, 2250–2261.

32 J. Zhang, M. E. Matta, M. A. Hillmyer, *ACS. Macro. Lett.* **2012**, *1*, 1383–1387.

33 C. Zhang, L. Li, S. Zheng, *Macromolecules* **2013**, *46*, 2740.

34 C. S. Daeffler, R. H. Grubbs, *Macromolecules* **2013**, *46*, 3288–3292.

35 L. E. Rosebrugh, V. M. Marx, B. K. Keitz, R. H. Grubbs, *J. Am. Chem. Soc.* **2013**, *135*, 10032–10035.

36 K. O. Kim, T. L. Choi, *Macromolecules* **2013**, *46*, 5905–5914.

37 S. Ohno, K. Sugiyama, Y. Koh, T. Tsujii, M. Fukuda, H. Yamahiro, Y. Oikawa, N. Yamamoto, K. Ootake, *Macromolecules* **2004**, *37*, 8517–8522.

38 L. Wang, S. Zheng. *Mater. Chem. Phys.* **2012**, *136*, 744.

39 Y. Zheng, L. Wang, R. Yu, S. Zheng, *Macromol. Chem. Phys.* **2012**, *213*, 458–469.

40 Y. Zheng, L. Wang, S. Zheng, *Euro. Polym. J.* **2012**, *48*, 945–955.

41 M. R. Buchmeiser, In Handbook of Ring-Opening Polymerization, 1st ed.; P. Dubois, C. Olivier, and J. Raquez, Eds.; Wiley-Interscience: Weinheim, **2009**; Vol. *1*, p 197.

42 M. Wathier, S. S. Stoddart, M. J. Sheehy, M. W. Grinstaff, *J. Am. Chem. Soc.* **2010**, *132*, 15887–15889.

43 M. R. Buchmeiser, In Synthesis of Polymers: New Structures and Methods, 1st ed.; A. D. Schlouter and C. J. Hawker, Eds.; Wiley-Interscience: New York, **2012**; Vol. *1*, p 547.

44 B. K. Keitz, A. Fedorov, R. H. Grubbs, *J. Am. Chem. Soc.* **2012**, *134*, 2040–2043.

45 C. P. Radano, O. A. Scherman, N. Stingelin-Stutzmann, C. Müller, D. W. Breiby, P. Smith, R. A. Janssen, E. Meijer, *J. Am. Chem. Soc.* **2005**, *127*, 12502–12503.

46 R. Bandari, T. Höche, A. Prager, K. Dirnberger, M. R. Buchmeiser, *Chem. Eur. J.* **2010**, *16*, 4650–4658.

47 D. Bek, N. Žilková, J. Dědeček, J. Sedláček, H. Balcar, *Top. Catal.* **2010**, *53*, 200–209.

48 F. Sinner, M. R. Buchmeiser, *Macromolecules* **2000**, *33*, 5777–5786.

49 C. W. Bielawski, D. Benitez, R. H. Grubbs, *J. Am. Chem. Soc.* **2003**, *125*, 8424–8425.

50 J. Zhang, M. E. Matta, H. Martinez, M. A. Hillmyer, *Macromolecules* **2013**, *46*, 2535–2543.

51 D. M. Lynn, S. Kanaoka, R. H. Grubbs, *J. Am. Chem. Soc.* **1996**, *118*, 784–790.

52 H. D. Maynard, S. Y. Okada, R. H. Grubbs, *Macromolecules* **2000**, *33*, 6239–6248.

53 K. H. Yoon, K. O. Kim, M. Schaeffer, D. Y. Yoon. *Polymer.* **2012**, *53*, 2290.

54 P. D. Zeits, T. Fiedler, J. A. Gladysz. *Chem. Commun.* **2012**, *48*, 7925–7927.

55 W. R. Lian, H. Y. Wu, K. L. Wang, D. J. Liaw, K. R. Lee, J. Y. Lai. *J. Polym. Sci. Part A: Polym. Chem.* **2011**, *49*, 3673–3680.

56 D. F. Sedbrook, D. W. Paley, M. L. Steigerwald, C. Nuckolls, F. R. Fischer, *Macromolecules* **2012**, *45*, 5040–5044.

57 P. O'Rourke-Muisener, C. Jalbert, C. Yuan, J. Baezold, R. Mason, D. Wong, Y. Kim, J. Koberstein, B. Gunesin, *Macromolecules* **2003**, *36*, 2956–2966.

58 J. Koberstein, *J. Polym. Sci. Part B: Polym. Phys.* **2004**, *42*, 2942–2956.

59 D. Kaelble, K. Uy. *J. Adhes.* **1970**, *2*, 66–81.

60 D. Kaelble, Physical Chemistry of Adhesion. Wiley-Interscience: New York, **1971**.

61 A. Adamson, Physical Chemistry of Surfaces, 5th ed.; Wiley Interscience: New York, **1990**.

62 L. M. Pitet, M. A. Hillmyer, *Macromolecules* **2009**, *42*, 3674–3680.

63 Y. Ni, S. Zheng, *J. Polym. Sci. Part A: Polym. Chem.* **2007**, *45*, 1247–1259.

64 S. Iwayanagi, I. Sakurai, T. Sakurai, *J. Macromol. Sci. B: Phys.* **1968**, *B2*, 163–177.

65 T. Tatsumi, T. Fukushima, K. Imada, M. Takayanagi, *J. Macromol. Sci. B: Phys.* **1967**, *B1*, 459–483.